Int J Clin Exp Med 2022;15(3):78-96
www.ijcem.com /ISSN:1940-5901/IJCEM0136682

Original Article

Differential proteins in alveolar macrophages in patients with different stages of silicosis

Yihong Gong[1*], Huan Wang[1*], Linhui Kan[1], Yali Tang[1], Shuyu Xiao[2], Yuping Bai[1], Nan Liu[1], Chunyan Meng[1], Huisheng Qi[3], Fuhai Shen[1]

[1]Hebei Province Key Laboratory of Occupational Health and Safety for Coal Industry, School of Public Health, North China University of Science and Technology, Tangshan 063210, Hebei, China; [2]Tangshan Center of Disease Control and Prevention, Tangshan 063000, Hebei, China; [3]Tangshan City Workers' Hospital, Tangshan 063000, Hebei, China. [*]Equal contributors.

Received June 23, 2021; Accepted December 26, 2021; Epub March 15, 2022; Published March 30, 2022

Abstract: Objective: In order to obtain proteins related with the occurrence and development of silicosis and further reveal the development mechanism of silicosis, we collected alveolar macrophages from lung lavage fluid of silicosis patients, and studied the different proteins in alveolar macrophages of silicosis patients at different stages. Methods: A total of 31 patients with silicosis were selected who were male and who were exposed to dust, or dust removal within 2 years prior to our study. Two-dimensional gel electrophoresis was used to isolate the differential proteins. Image Master 2D Platinum software was used to identify differential protein spots. This method was used to identify differential spots, namely New ultrafleXtreme reflective tandem matrix assisted laser desorption time of flight mass spectrometry. GO, KEGG Pathway and PPI analysis of differential proteins were carried out by bioinformatics. Results: Through bioinformatics analysis, we found that these differential proteins mainly participate in the pathway of fatty acid degradation, valine, leucine and isoleucine degradation, lysine degradation, tryptophan metabolism, pyruvate metabolism, metabolic pathways, etc. Bioinformatics analysis showed that there were interactions between ECHS1 and ALDH2. Conclusions: Using differential proteomics, we found that the proteins associated with silicosis development in alveolar macrophages were ANXA4, PRDX4, ERP29, KRT10, FTL, ECHS1, and ALDH2; the findings of which enriched the alveolar macrophage protein library of silicosis. Through bioinformatics analysis, the main mechanisms of pulmonary alveolar macrophages involved in the development of silicosis were fatty acid metabolism, MAPK activity regulation, oxidative stress, notch signaling pathway, and negative regulation of interleukin-8 secretion. The expression of ECHS1 protein in the pulmonary dust deposition group was different from the silicosis groups of grade one and two. ECHS1 may be the key protein in the development of silicosis.

Keywords: Bioinformatics, silicosis, proteomics

Introduction

Pneumoconiosis is one of the most prominent occupational disease that threatens the health of workers. It is reported that hundreds of millions of workers who are exposed to dust face the risk of pneumoconiosis, and it has a high prevalence and incidence in developing countries [1-4]. In recent years, the incidence of pneumoconiosis in China has been high, even increasing annually. The government and health departments are aware of the pain and issues that workers with pneumoconiosis have to face. In order to deal with this severe situation, the government has invested a lot of manpower and material resources to identify and aid pneumoconiosis patients and to enable them to receive effective treatment. It is very necessary to study pneumoconiosis in order to find new ideas and methods for its prevention, treatment and rehabilitation [5, 6].

Through understanding the genome, research on the pathogenesis and biomarkers of pneumoconiosis has gradually increased, and some achievements have been made [7, 8]. After years of study, scholars have identified inflammatory factors, such as tumor necrosis factor, interleukin, inflammatory chemokines related to silicosis, etc. The results of which have re-

vealed a possible pathogenesis theory of pneumoconiosis and created the "eight words policy" for prevention and treatment of pneumoconiosis, which plays an important guiding role in determining the etiology of pneumoconiosis and may help to eventually eliminate pneumoconiosis completely.

As the basic unit for cell function execution and the direct embodiment of life activities, proteins participate in regulating almost all life activities of the living organisms, and they control growth, development, reproduction, energy metabolism, and the stress response, etc. Proteomics is characterized by its high throughput analysis, with high pertinence, systematization and integration of results. Compared with the detection of a single biological index, the research complexity of this method is greatly increased. Proteomics can reveal biological phenomena closely to the real life situation. Many major diseases with unclear mechanisms, such as various cancers, diabetes, and silicosis, have been better understood through continuous research. But this does not comprehensively evaluate the occurrence and development of the disease from its overall perspective. Therefore, proteomics is widely used in the study of major diseases which have unknown mechanisms.

We wanted to compare the major protein expression types of silicosis development in macrophages extracted from lung lavage fluid of silicosis patients (GBZ 70-2015) and pneumoconiosis patients by differential proteomics. The purpose of this study was to obtain protein factors related to the occurrence and development of silicosis, and to provide clues to the mechanism of silicosis, as well as the basis for its prevention and treatment.

Methods

Subjects

We selected subjects from pneumoconiosis patients, who had a simple history of dust exposure, who were only exposed to rock dust. There were no other diseases involved as much as possible, such as fatty liver, kidney stone, hypertension, diabetes, etc. The subjects were male workers who had been exposed to dust (within the last 2 years). The subjects of study were those who were diagnosed as having silicosis by the local pneumoconiosis diagnostic expert group according to the Diagnosis of Occupational Pneumoconiosis (GBZ 70-2015) in China and those who were not diagnosed with silicosis but who had a dust collection history such as dust deposition in the lung, excluding other fibrotic diseases, pulmonary inflammatory diseases, tuberculosis and hepatitis B.

According to expert diagnosis and treatment results, the subjects were divided into four groups: pulmonary dust deposition group, stage I silicosis group, stage II silicosis group, and stage III silicosis group; with 5, 10, 9 and 7 people in each group. There were no differences in age and body mass index among the groups. Before collecting the lavage fluid, patients signed the informed consent form, and this study applied to the Medical Ethics Committee of North China University of Science and Technology for approval.

Interpretation of the basic data of the selected subjects in the experiment

We analyze the distribution of the following indicators among each group in detail to ensure the comparability among the research subjects of each group.

Exercise habit: Less exercise was defined as having no other form of exercise other than taking part in work activities. Exercise at any intensity of not less than 3 times per week, each time of not less than 30 min, was defined as occasional exercise. Exercise at any intensity more than three times a week, each time not less than 30 min, was defined as regular exercise.

Region: Geographically boundary of the Qinling Mountains-Huaihe River line, south was defined as the south, north was defined as the north. A total of 17 patients from the southern provinces and a total of 14 patients from the Northern provinces were enrolled.

Smoking history: According to the WHO definition of smoking, the history of smoking was defined as continuous or accumulated smoking for more than 6 months.

Drinking history: Drinking alcohol twice a week or more often, at 50 g or more each time for six months was defined as having a drinking history.

Dust exposure time (year): Time spent in dust related work (rock drilling, development, mining, comminution, transportation, etc.).

Dust removal time (year): Time of leaving dust related work (rock drilling, development, mining, crushing, transportation, etc.).

Dust properties: In this study, according to the dust exposure history data of the investigated silicosis patients, the contact coal mine rock dust, stone grinding rock dust, quartz sand, boron mine rock dust, carboniferous mine rock dust, phosphate rock dust and fluorite mine rock dust were defined as non-metallic mine dust. The iron ore dust, gold ore dust, molybdenum ore dust, lead-zinc ore dust, barite ore dust, tungsten ore dust, tin ore dust and manganese ore dust were defined as metal ore dust. Contact with both metallic and non-metallic mineral dust was defined as mixed dust.

COPD: The subjects with FEV1/FVC≥70% were defined as having no COPD based on their vital capacity. Patients with FEV1/FVC<70% and with or without chronic cough and expectoration were defined as having COPD.

Sample preparation

We collected the first eight samples of lung lavage fluid from each subject, about 4000 ml, from four groups of subjects: pulmonary dust deposition group, stage I silicosis group, stage II silicosis group, stage III silicosis group. The first 7 samples and the eighth were treated separately. They were filtered with 4 layers of sterile gauze and centrifuged for 15 minutes at 1500 rpm. We rinsed the cells with pre cooled pre-cooled PBS, and collected cell precipitation. The first 7 samples of cells were inoculated into a 10 cm culture dish containing 1640 culture medium, each plate containing 107 cells, and the eighth sample containing 106 cells/plate was inoculated into a 24-well plate containing 1640 culture medium, and gently placed in a 37°C CO_2 incubator for 2 hours. Two hours later, the protein was extracted from the macrophages in a 10 cm culture dish. The process of protein extraction was as follows: Pour out the culture medium, rinse with PBS for 3 times; digest with pancreatic enzyme for 5 minutes. Add 3 ml of culture solution to each culture dish, transfer the cells of 2 culture dishes to a 15 ml centrifuge tube, and centrifuge at a speed of 1000 rpm for 5 minutes. The culture solution was poured out, and 6 ml PBS was added to each test tube for resuspension, and centrifugation was carried out for 5 minutes at a speed of 1000 rpm. The PBS was poured out, the remaining PBS was absorbed with absorbent paper, and 100 μL of cell lysate and protease inhibitor were added into each centrifugal tube. Transfer the above liquid to a 1.5 mL EP tube. Ultrasonication was performed intermittently in ice bath for 30 s, 500 W, for 1 s, at intervals of 2 s, and centrifuged at 4°C and 14000 r/min for 25 minutes, and the supernatant was collected and packed in EP tube, and stored at -80°C. The extraction process of protein was carried out on ice to reduce protein hydrolysis.

Two-dimensional gel electrophoresis

Detailed descriptions of the laboratory methods and statistical analysis were proposed by Bilal A et al. 2017 [9]. For two-dimensional gel electrophoresis, protein was solubilized in 450 L aqueous solution. IPG-strips (pH 3-10 nl) were rehydrated at 20°C with the protein extract. A 2.4 ml plastic strip slot cover liquid was added to the IPG plastic strip slot and covered with a plastic cover [10]. One-dimensional electrophoresis was started on the IPGphor electrode plate. SDS-PAGE gel was prepared, and second to SDS-PAGE gel electrophoresis was performed in Ettan DALT Twelve. It took 3 hours for Coomassie Brilliant Blue R-250 staining. The gel was repeatedly washed with decolorizing solution made of ethanol and acetic acid until the protein spots were clear and the background was bright. The gel was stored in 10% glycerin for 1 day and scanned by laboratory scanning and image scanner software. The gel analysis was carried out by The ImageMaster V 6.0 of GE. The volume% value of protein spots obtained was tested by Student's T-Test in the Excel. The protein spots at $P<0.05$ were selected as being differential protein spots, and the spots were removed from the gel using surgical blades and placed in 1.5 ml EP tubes to be detected by mass spectrometry.

Reflective tandem matrix assisted laser desorption time-of-flight mass spectrometry

The extracted differential protein spots were detected by Beijing Yipu Biotechnology Co., Ltd. using Bruker's New ultrafleXtreme type reflec-

Table 1. The general conditions of the research subject (n=31)

Factors		Dust deposition in the lungs (5, %)	Silicosis stage I (10, %)	Silicosis stage II (9, %)	Silicosis stage III (7, %)	χ^2	P
age	≤50	4 (80)	5 (50)	6 (67)	5 (71)	1.568	0.745
	>50	1 (20)	5 (50)	3 (33)	2 (29)		
area	North	3 (60)	5 (50)	2 (22)	4 (57)	2.902	0.467
	South	2 (40)	5 (50)	7 (78)	3 (43)		
smoking history	Have	4 (80)	6 (60)	8 (89)	6 (86)	2.463	0.499
	No	1 (20)	4 (40)	1 (11)	1 (14)		
drinking history	Have	1 (20)	4 (40)	4 (44)	2 (29)	1.122	0.841
	No	4 (80)	6 (60)	5 (56)	5 (71)		
dust exposure time (year)	≤10	1 (20)	3 (30)	4 (45)	5 (72)	6.847	0.332
	10~20	3 (60)	6 (60)	2 (22)	1 (14)		
	>20	1 (20)	1 (10)	3 (33)	1 (14)		
COPD	Have	1 (20)	5 (50)	2 (22)	4 (57)	3.156	0.394
	No	4 (80)	5 (50)	7 (78)	3 (43)		
dust properties	non-metal ore dust	4 (80)	3 (30)	6 (67)	5 (71)	7.529	0.208
	metal ore dust	0 (0)	6 (60)	2 (22)	2 (29)		
	mixed dust	1 (20)	1 (10)	1 (11)	0 (0)		
fatty liver	Have	0 (0)	1 (10)	2 (22)	0 (0)	2.226	0.670
	No	5 (100)	9 (90)	7 (78)	7 (100)		
Kidney stones	Have	2 (40)	6 (60)	5 (56)	1 (14)	3.980	0.274
	No	3 (60)	4 (40)	4 (44)	6 (86)		
Cardiovascular disease	Have	2 (40)	6 (60)	1 (11)	1 (14)	6.057	0.099
	No	3 (60)	4 (40)	8 (89)	6 (86)		

Note: Since n=31, the exact Fisher method is used, and the statistic is χ^2.

tive tandem matrix-assisted laser desorption time-of-flight mass spectrometry. The 2DE gel containing differential protein spots was first cut into about 1 mm^3, then 50% acetonitrile 25 mM NH_4HCO_3 was used to decolorize and freeze-dry the cut particles to complete the decolorization. Next we added 15 ng/ul (about 3-5 ul) trypsin solution and incubate for 1 h at 4°C. A certain volume of 25 mM NH_4HCO_3 was added until the colloidal particles were submerged. The enzymatic hydrolysis time in the water bath was 16 hours, and the temperature was 37°C. To this 5% TFA aqueous solution was added and a 37°C water bath was applied for 1 hour. Then it went in a 2.5% TFA/50% ACN 37°C water bath for 1 h to extract the digested polypeptide, and the extract was freeze-dried to achieve enzymatic hydrolysis in the gel. The protein was identified by time of flight mass spectrometry and Swissprot 57.15.

Bioinformatics

Bioinformatics is a type of conceptual biology in the field of macromolecules. This is an interdisciplinary subject related to medicine, biology, genomics, genetics, physiology, mathematics and computer science, which came along with the Human Genome Project. It is used for understanding and organizing information related to biological macromolecules [11].

GO (Gene Ontology) analysis application DAVID (https://david.ncifcrf.gov/) website analysis [12] was used. GO analysis includes 3 modules: differentially expressed protein biological process, molecular function, and cellular component. GO analysis was performed in https://david.ncifcrf.gov/summary.jsp. KEGG (Kyoto Encyclopedia of Genes and Genomes) pathway analysis used http://www.kegg.jp/website analysis, where each protein was entered to analyze its route [13]. PPI (protein-protein interaction) analysis of protein interactions was performed on the https://string-db.org/cgi/input.pl website to establish a protein interaction network [14].

Results

The baseline characteristics of the study population were shown in **Table 1**. We studied the factors affecting the progression of pneumoco-

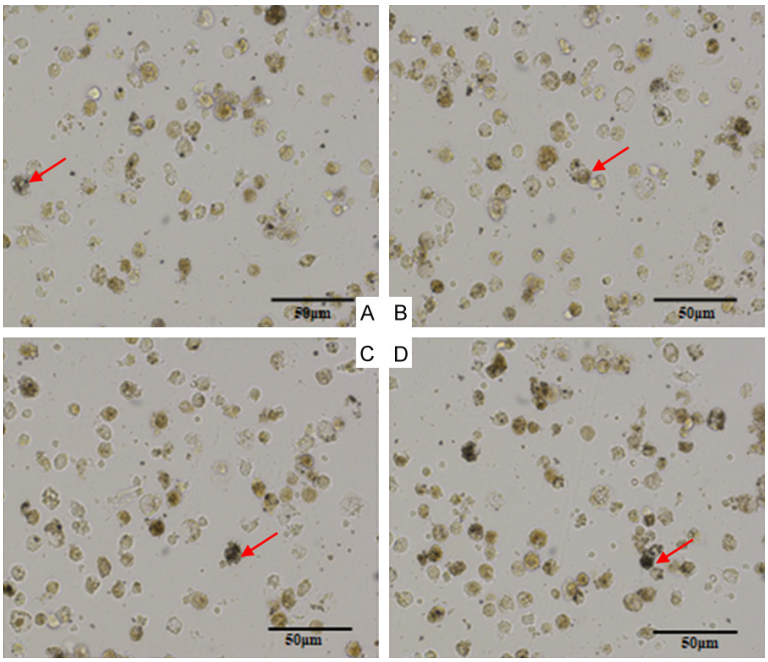

Figure 1. The macrophage morphology of silicosis. Note: A. The pulmonary dust deposition group. B. The silicosis stage I group. C. The silicosis stage II group. D. The silicosis stage III group. The scale bar was 50 μm. Arrows indicated swallowing macrophages (×400).

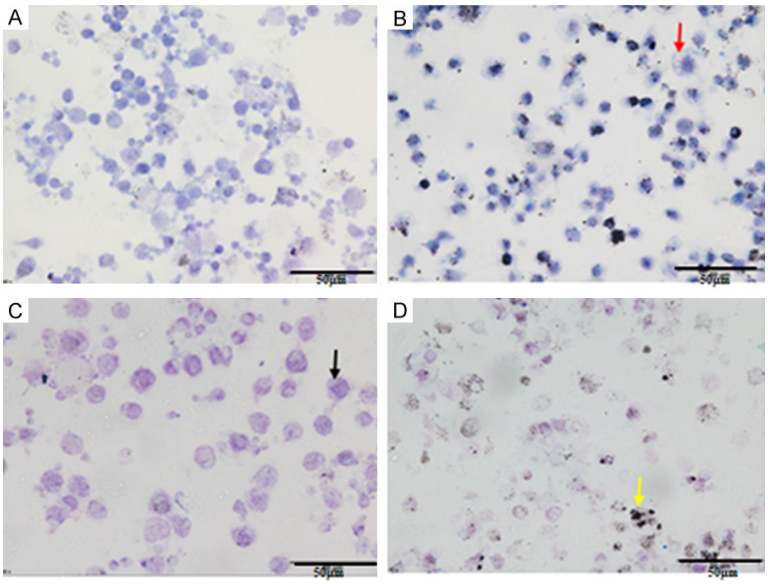

Figure 2. The ray-giemsa stained of alveolar macrophage. Note: A. Alveolar lavage macrophages from patients with dusty lung disease. B. Alveolar lavage macrophages from patients with silicosis stage I. C. Alveolar lavage macrophages of patients with silicosis stage II. D. Alveolar lavage macrophages of patients with silicosis stage III. The scale bar was 50 μm. The red arrow pointed to the vacuole, the black arrow pointed to the nucleus, and the yellow arrow pointed to dust (×400).

niosis, such as age, region, smoking history, drinking history, exposure time, dust properties, chronic obstructive pulmonary disease (COPD), fatty liver, kidney stone and cardiovascular and cerebrovascular diseases, etc., and carried out statistical analysis. In order to obtain the distribution of various risk factors in the four groups, they were defined as the pulmonary dust deposition group, the stage I silicosis group, the stage II silicosis group, and the stage III silicosis group.

The basic data included 31 silicosis patients in this experiment, after chi-square test, the above ten risk factors that may have affected the progress of silicosis were evenly distributed among the four groups. In addition, in order to avoid the influence of different nationalities on the results of proteomics, the 31 silicosis patients were all Han nationality. The 31 patients with silicosis were homogeneous, and as such could be used for the comparative study of differential proteins between different populations.

Alveolar macrophage morphology in lung lavage fluid of silicosis patients

After 2 hours of culture, macrophages in lung lavage fluid showed good adhesion and growth, and some macrophages protruded from the pseudopod. Most macrophages engulfed a large amount of dust, such as the alveolar macrophages indicated by the arrows, and the dust had almost filled the entire macrophages (**Figure 1**). Some macrophages eventually ruptured and broke down due to engulfing a large amount of dust. According to the culture condition, the adhesion of macrophages in the pulmonary dust

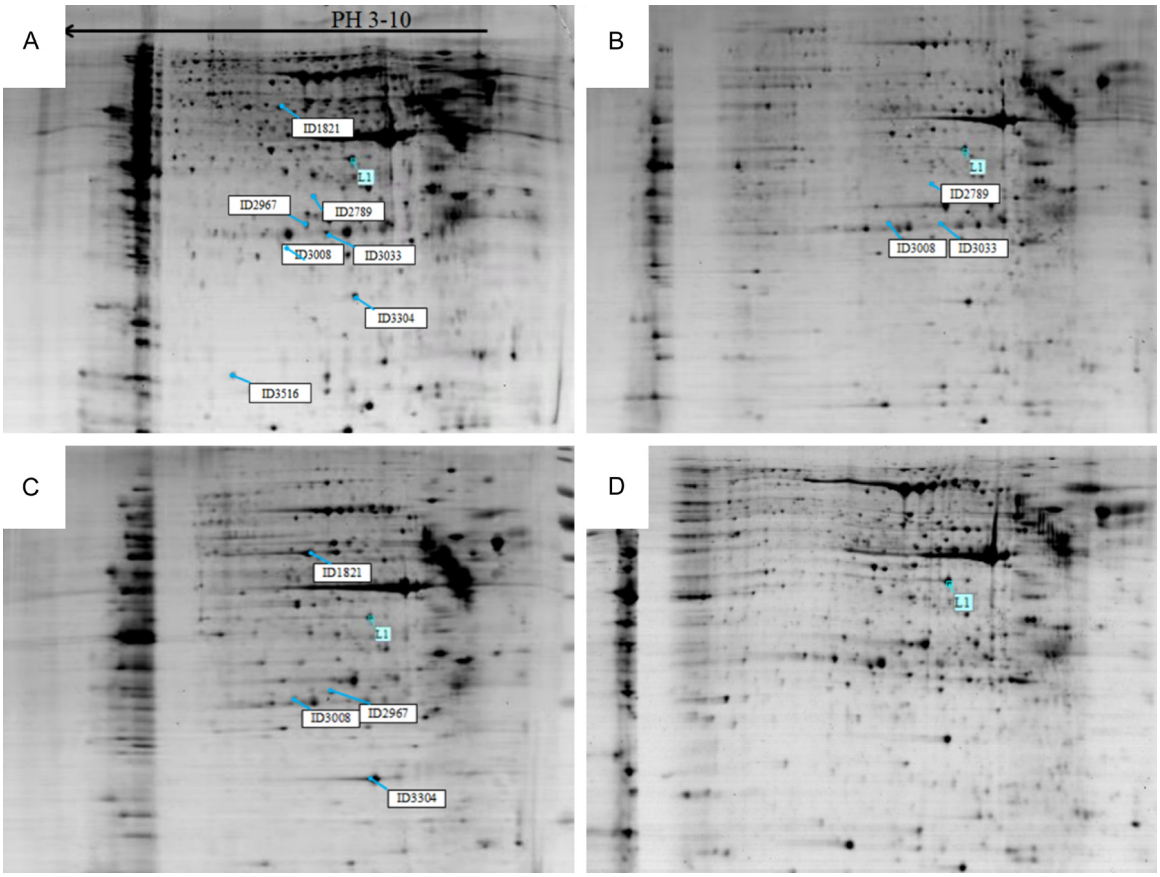

Figure 3. The protein speckle pattern of two-dimensional gel electrophoresis. Note: A. The macrophage protein spot map of lung lavage fluid from patients with pulmonary dust deposition; B. Macrophage protein spot map of lung lavage fluid of silicosis stage I silicosis; C. Macrophage protein spot map of lung lavage fluid of silicosis stage II silicosis; D. The macrophage protein spot map of lung lavage fluid in patients with stage III silicosis.

deposition group was the strongest, while that in the stage III silicosis group was not as good as that in the light-stage group.

Macrophages in the lung lavage fluid were seeded into 24-well plates with a certain concentration, and then cultured in a CO_2 incubator for 2 hours. After fixation with paraformaldehyde, Wright's Giemsa staining was performed to determine the morphology of alveolar macrophages in 4 patients with pneumoconiosis. In the field of view, the nucleus could be seen in the shape of a horseshoe distributed on both ends of the cell, and some cells had multiple nuclei, as indicated by the black arrow. As the aggravation of silicosis, the cytoplasmic component increased, and the nucleus was squeezed to become smaller. Unstained vacuoles could be seen in the field of vision, and the red arrow pointed to the location, and the heavier the period, the more vacuoles. After staining, dark brown dust clumps were still unstained, as indicated by yellow arrows (**Figure 2**).

Two-dimensional gel electrophoresis differential protein spots

The pH value of the adhesive tape was 3-10 NL, and the color mark indicates the range of 10-170 KDa. According to the identification and analysis of Image Master v 6.0 software, 1500 protein spots were matched in 4 gels of the pulmonary dust deposition group. A total of 4619 protein spots were matched with 9 gels in stage I silicosis group. In the stage II silicosis group, 3049 protein spots were matched with 8 gels. In the stage III silicosis group, 4,713 protein spots were matched with 6 gels (**Figure 3**).

As shown in **Table 2**. The pulmonary dust syndrome group overlapped in 17 differential protein spots with the celiac group, the pulmonary

Table 2. The conditions of diverse protein spots

Factors	S0 vs S1	S0 vs S2	S0 vs S3
Identify the number of difference points	17	28	6
Number of mass spectrometry identifications	6	11	6
Identification of the number of difference points	2	5	0

Note: S0 represented the pneumoconiosis group of lung, S1 represented the stage silicosis group, S2 represented the stage silicosis group, and S3 represented the stage silicosis group.

dust syndrome group overlapped in 28 differential protein spots between the pulmonary dust-synostic group and the celiac group, and the pulmonary dust-destooma group overlapped in six different protein spots. There were 6 differential protein spots between the pulmonary dust deposition group and the stage silicosis group, and the match IDs were 3033, 2789, 2726, 2649, 3207 and 3008. There were a total of 11 differential protein spots between the pulmonary dust deposition group and the stage II silicosis stage for diarrhea, and the match IDs were 3516, 3304, 2276, 1792, 3008, 1821, 2967, 2805, 2376, 1857 and 1349. There were 6 differential protein spots between the pulmonary dust deposition group and the stage III silicosis group, and the match IDs were 2828, 2863, 3681, 3704, 2959 and 2965. A total of 23 spots were identified by mass spectrometry. Interestingly, the differential protein spot with Match ID of 3008 was different in both the pulmonary dust deposition group and the stage I silicosis group, and the pulmonary dust deposition group and the stage II silicosis group, and it might be the key protein for the occurrence and development of silicosis.

Mass spectrometry results

The basic principle of mass spectrometry is to give a certain field strength of a protein, to break it into charged fragments and move them to a certain length of field strength. First-order mass spectrometry can detect all charged parent ion fragments. On the basis of the first-order mass spectrometry, the second-order mass spectrometry can further break down the parent ion fragments into smaller fragments to detect all the product ion fragments. In this experiment, the extracted differential protein spots were detected by Beijing Yipu Biotechnology Co., Ltd. using Bruker's New ultrafleXtreme reflective tandem matrix-assisted laser desorption time-of-flight mass spectrometry. The reflection mode scan range was 900-4000 Da. As shown in **Figure 4**, the abscissa was the mass-to-charge ratio and the ordinate was the intensity of the fragment. It can be seen that the mass-to-charge ratio of the secondary mass spectrum was significantly smaller than that of the primary mass spectrum. Generally, the results of the secondary mass detection and identification were more accurate.

The fragments identified by mass spectrometry were searched and compared in the SwissProt 57.15 (515203 sequences; 18133-4896 residues) database. The search score limit was 30, $P<0.05$. Seven human proteins of ANXA4, PRDX4, ERP29, KRT10, FTL, ECHS1, and ALDH2 were identified through search and comparison. Their scores were 753, 999, 380, 880, 742, 315, and 355, respectively.

Mass spectrometry results were retrieved from the SwissProt 57.15 database (**Figure 5**). The set score was 43. $P<0.05$ was statistically significant and could be used to identify a certain protein. By searching and matching, the Match ID is 3033 and the protein spot score was 753, which was much larger than the set 43. Therefore, it could be determined that the Match ID 3033 protein spot was a human-derived ANXA4 protein.

After analysis with Image Master v6.0 software and t-test with uneven variance, the differential protein points obtained were cut out. They were compared with the new UltrafleXtreme reflection tandem matrix-assisted laser desorption time-of-flight mass spectrometry with the SwissProt 57.15 database, and we identified two different proteins in the pulmonary dust deposition group and the stage I silicosis group, namely, membrane annexin A4 (ANXA4) and recombinant human peroxide reductase 4 (PRDX4). There were five proteins in the pulmonary dust deposition and the stage I silicosis group, namely endoplasmic reticu-

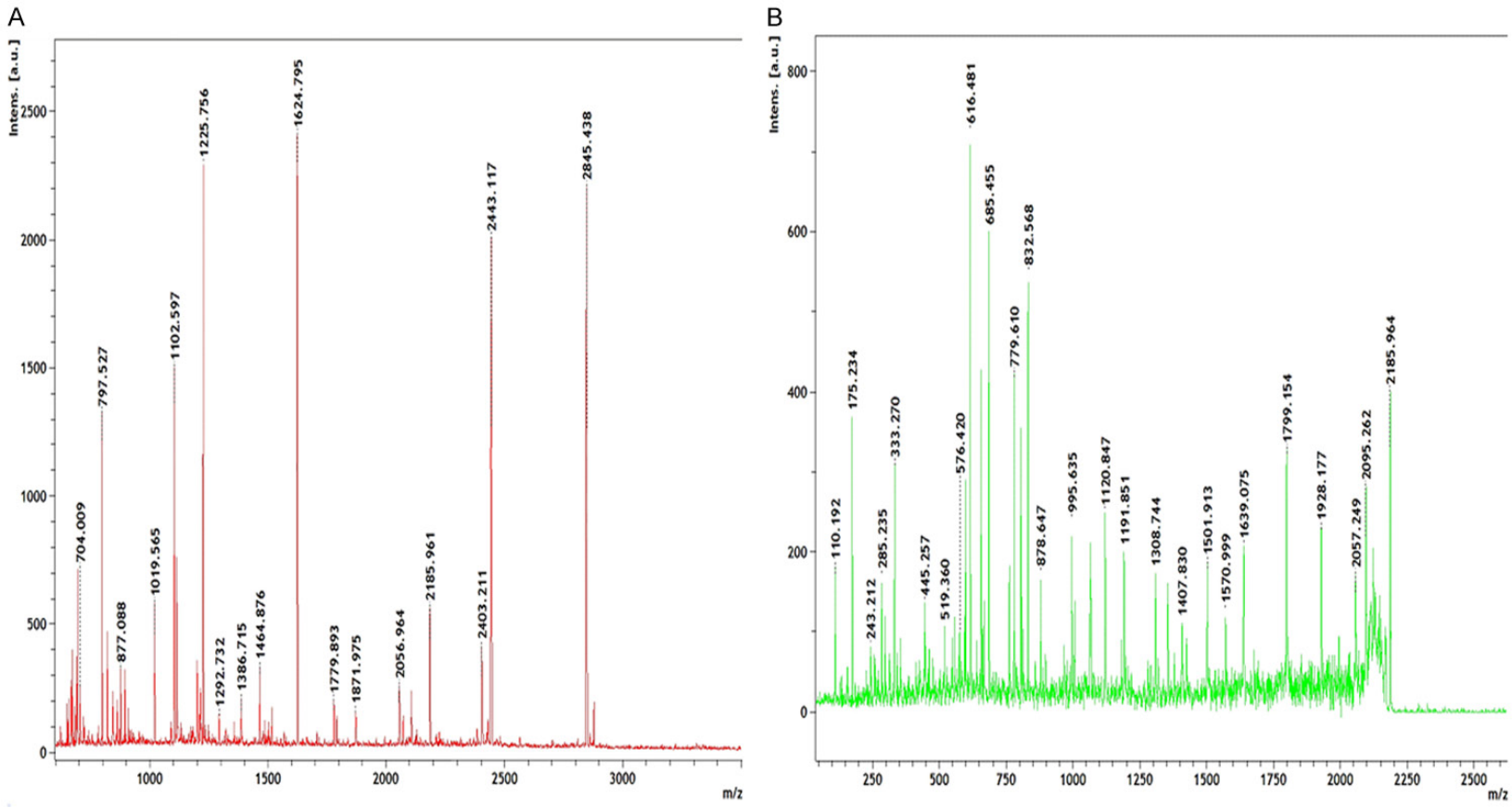

Figure 4. The figure of the mass spectrum. Note: A. The primary spectrum; B. The secondary spectrum.

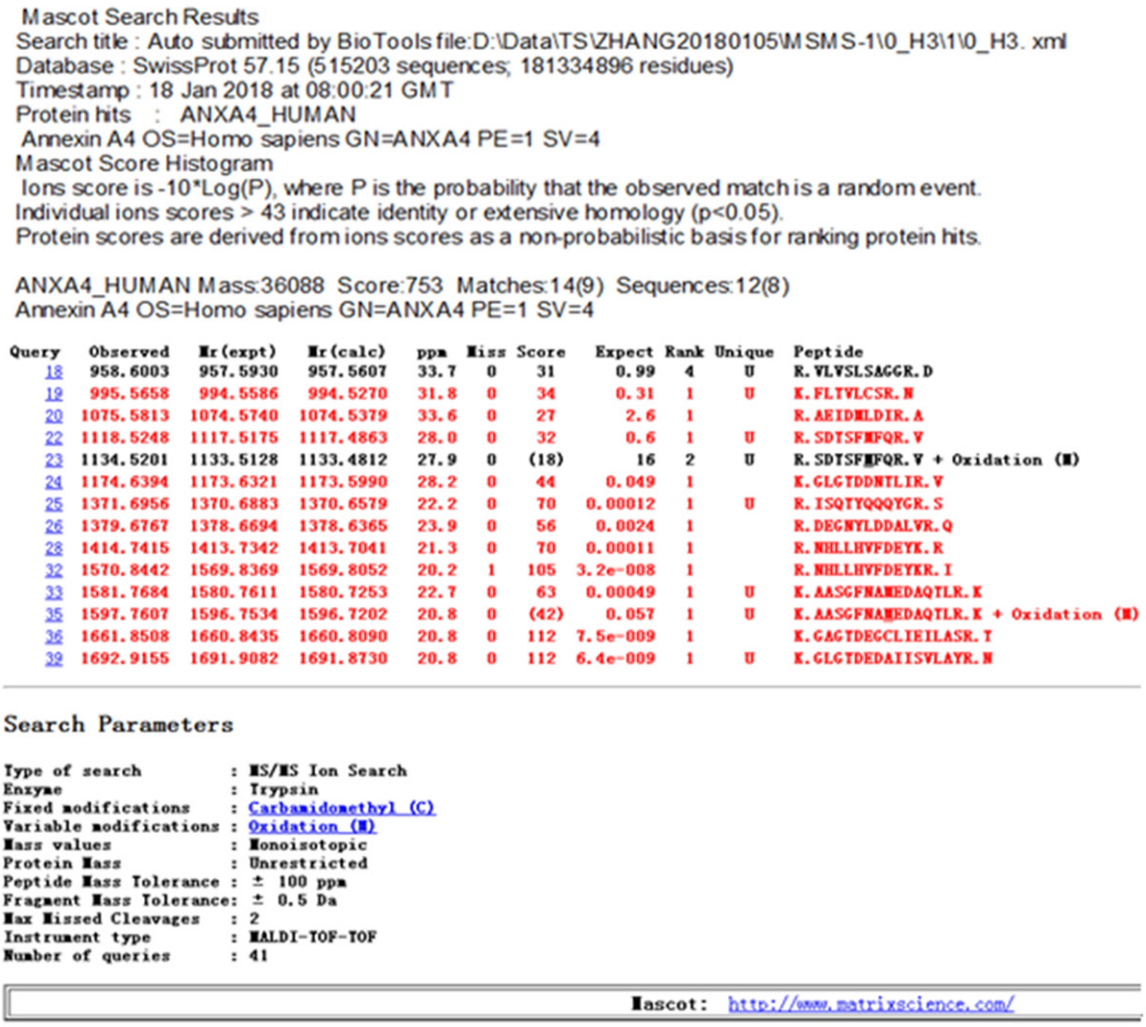

Mascot Search Results
Search title : Auto submitted by BioTools file:D:\Data\TS\ZHANG20180105\MSMS-1\0_H3\1\0_H3. xml
Database : SwissProt 57.15 (515203 sequences; 181334896 residues)
Timestamp : 18 Jan 2018 at 08:00:21 GMT
Protein hits : ANXA4_HUMAN
Annexin A4 OS=Homo sapiens GN=ANXA4 PE=1 SV=4
Mascot Score Histogram
Ions score is -10*Log(P), where P is the probability that the observed match is a random event.
Individual ions scores > 43 indicate identity or extensive homology (p<0.05).
Protein scores are derived from ions scores as a non-probabilistic basis for ranking protein hits.

ANXA4_HUMAN Mass:36088 Score:753 Matches:14(9) Sequences:12(8)
Annexin A4 OS=Homo sapiens GN=ANXA4 PE=1 SV=4

Query	Observed	Mr(expt)	Mr(calc)	ppm	Miss	Score	Expect	Rank	Unique	Peptide
18	958.6003	957.5930	957.5607	33.7	0	31	0.99	4	U	R.VLVSLSAGGR.D
19	995.5658	994.5586	994.5270	31.8	0	34	0.31	1	U	K.FLTVLCSR.N
20	1075.5813	1074.5740	1074.5379	33.6	0	27	2.6	1		R.AEIDMLDIR.A
22	1118.5248	1117.5175	1117.4863	28.0	0	32	0.6	1	U	R.SDTSFMFQR.V
23	1134.5201	1133.5128	1133.4812	27.9	0	(18)	16	2	U	R.SDTSFMFQR.V + Oxidation (M)
24	1174.6394	1173.6321	1173.5990	28.2	0	44	0.049	1		K.GLGTDDNTLIR.V
25	1371.6956	1370.6883	1370.6579	22.2	0	70	0.00012	1	U	R.ISQTYQQQYGR.S
26	1379.6767	1378.6694	1378.6365	23.9	0	56	0.0024	1		R.DEGNYLDDALVR.Q
28	1414.7415	1413.7342	1413.7041	21.3	0	70	0.00011	1		R.NHLLHVFDEYK.R
32	1570.8442	1569.8369	1569.8052	20.2	1	105	3.2e-008	1		R.NHLLHVFDEYKR.I
33	1581.7684	1580.7611	1580.7253	22.7	0	63	0.00049	1	U	K.AASGFNAMEDAQTLR.K
35	1597.7607	1596.7534	1596.7202	20.8	0	(42)	0.057	1	U	K.AASGFNAMEDAQTLR.K + Oxidation (M)
36	1661.8508	1660.8435	1660.8090	20.8	0	112	7.5e-009	1		K.GAGTDEGCLIEILASR.T
39	1692.9155	1691.9082	1691.8730	20.8	0	112	6.4e-009	1	U	K.GLGTDEDAIISVLAYR.N

Search Parameters

Type of search : MS/MS Ion Search
Enzyme : Trypsin
Fixed modifications : Carbamidomethyl (C)
Variable modifications : Oxidation (M)
Mass values : Monoisotopic
Protein Mass : Unrestricted
Peptide Mass Tolerance : ± 100 ppm
Fragment Mass Tolerance: ± 0.5 Da
Max Missed Cleavages : 2
Instrument type : MALDI-TOF-TOF
Number of queries : 41

Mascot: http://www.matrixscience.com/

Figure 5. The spectrometry retrieval results for Match ID 3033 by MALDI-TOF-TOF mass.

Table 3. The mass spectrometry detection results of Protein spots

Match ID	Abbreviation of protein name	Full name of protein	Comparative Group
3033	PRDX4	Peroxiredoxin-4	Pulmonary dust deposition and stage I
2789	ANXA4	Annexin A4	Pulmonary dust deposition and stage I
3516	KRT10	Keratin, type I cytoskeletal 10	Pulmonary dust deposition and stage II
3304	FTL	Ferritin light chain	Pulmonary dust deposition and stage II
3008	ECHS1	Enoyl-CoA hydratase	Pulmonary dust deposition and stage II
2967	ERP29	Endoplasmic reticulum resident protein 29	Pulmonary dust deposition and stage II
1857	ALDH2	Aldehyde dehydrogenase, mitochondrial	Pulmonary dust deposition and stage II

lum protein 29 (ERP29), keratin type I cytoskeleton (KRT10), ferritin light chain (FTL), and mitochondrial enoyl-coenzyme A hydratase (ECHS1) and mitochondrial acetaldehyde dehydrogenase (ALDH2) (**Table 3**).

Bioinformatics analysis

The bioinformatics analysis of seven proteins identified by mass spectrometry was carried out. By labeling the function of each protein

with bioinformatics, we found the signal pathways involved with the seven proteins and their relationship with the occurrence and development of silicosis, and establish the interaction network of the seven proteins (**Tables 4**, **5**).

The biological processes of the ANXA4 gene included Notch signaling pathway, epithelial differentiation, negative regulation of NF-κB transcription factor activity, negative regulation of apoptosis, negative regulation of catalytic activity, negative regulation of IL-8 secretion, RNA polymerase II, signal transduction [15]. Cell location: cell membrane, cytoplasm, extracellular matrix, nucleus and nuclear membrane, plasma membrane, vesicle membrane. The molecular functions were: NF-κB binding, calcium ion binding, calcium dependent phospholipid binding, binding, calcium dependent protein binding, the same protein binding, phospholipase inhibitor activity.

The biological processes of PRDX4 gene included: 4-hydroxyproline metabolism, I-kβ phosphorylation, cell redox homeostasis, cell oxidative detoxification, extracellular matrix, male gonad development, as well as negative regulation of male germ cell proliferation, neutrophil degranulation, redox process, protein maturation through protein folding, active oxygen metabolism and spermatogenesis.

The biological processes of the ERP29 gene included MAPK activation, negative regulatory gene expression [16], negative regulatory protein secretion, positive regulatory gene expression, positive regulatory protein phosphorylation, protein folding and unfolding, protein secretion, endoplasmic reticulum stress regulating internal apoptosis signal pathway. Cell localization: cell membranes, endoplasmic reticulum, endoplasmic reticulum cavity, extracellular matrix, melanosome, smooth endoplasmic reticulum and transport vesicles. The molecular functions was chaperone binding, rather than protein disulfide isomerase activation [17].

The biological processes of the KRT10 gene included keratinization, keratinization, keratinocyte differentiation and peptide cross-linking. Cell localization: cytoplasm, extracellular matrix, intermediate filament, membrane and nucleus. The molecular functions were: the structure and composition of epidermis [18].

The biological processes of the FTL gene included: iron homeostasis, iron homeostasis, iron homeostasis and neutrophil degranulation. Cell localization: autophagic vesicles, particle lumen of aniline blue, cytoplasm, extracellular matrix, intracellular ferritin complex, membrane. The molecular functions were: iron binding, protein binding, iron ion binding and protein binding.

The biological process of the ECHS1 gene was fatty acid β oxidation. Cell localization: extracellular matrix, mitochondrial matrix, mitochondria. The molecular functions were: enoyl COA hydratase activation, protein linkage.

The biological processes of the ALDH2 gene included: alcohol metabolism, carbohydrate metabolism, electron transport chain, ethanol decomposition, ethanol oxidation and fatty acid β oxidation. Cell localization: extracellular matrix, mitochondrial matrix. Molecular functions included: DNA linkage, activity of aldehyde dehydrogenase (NAD), activity of aldehyde dehydrogenase (P) + and activity of electron transfer.

ERP29 participates in the pathway of protein production in the endoplasmic reticulum. FTL was involved in the pathway of mineral absorption. ALDH2 was involved in the following pathways: glycolysis and glycogenesis, pentose and glucuronide mutualism, ascorbate metabolism, fatty acid degradation, valine, leucine and isoleucine degradation, lysine degradation, arginine and proline metabolism, histidine metabolism, tryptophan metabolism, β alanine metabolism, glycolipid metabolism, pyruvate metabolism, and metabolic pathways. The pathways involved in ECHS1 were: fatty acid elongation, fatty acid degradation, valine, leucine and isoleucine degradation, lysine degradation, tryptophan metabolism, β alanine metabolism, alanine metabolism, methyl butyrate metabolism, metabolic pathway, carbon metabolism, fatty acid metabolism. ALDH2 and ECSH1 were both involved in fatty acid degradation, valine, leucine and isoleucine degradation, lysine degradation, tryptophan metabolism, acetonate metabolism and metabolic pathways.

There were 17 nodes in the protein-protein interaction network, with an average score of 4.24. The *p*-value of PPI abundance was 2.4e-

Table 4. Differences proteins in gene ontology

Match ID	Gene Name	Species	GOTERM_BP_DIRECT	GOTERM_CC_DIRECT	GOTERM_MF_DIRECT
2789	ANXA4	Homo sapiens	GO:0006357~regulation of transcription from RNA polymerase II promoter, GO:0007165~signal transduction, GO:0007219~Notch signaling pathway, GO:0030855~epithelial cell differentiation, GO:0032088~negative regulation of NF-kappaβ transcription factor activity, GO:0043066~negative regulation of apoptotic process	GO:0005634~nucleus, GO:0005737~cytoplasm GO:0005886~plasma membrane, GO:0009986~cell surface, GO:0012506~vesicle membrane, GO:0031965~nuclear membrane, GO:0048471~perinuclear region of cytoplasm, GO:0070062~extracellular exosome	GO:0004859~Phospholipase inhibitor activity, GO:0005509~calcium ion binding, GO:0005515~protein binding, GO:0005544~calcium-dependent phospholipid binding, GO:0042802~identical protein binding, GO:0048306~calcium-dependent protein binding, GO:0051059~NF-kappaβ binding
2789	ANXA4	Homo sapiens	GO:0043086~negative regulation of catalytic activity, GO:0050819~negative regulation of coagulation, GO:2000483~negative regulation of interleukin-8 secretion		
3033	PRDX4	Homo sapiens	GO:0007252~I-kappaβ phosphorylation, GO:0007283~spermatogenesis, GO:0008584~male gonad development, GO:0019471~4-hydroxyproline metabolic process, GO:0022417~protein maturation by protein folding, GO:0030198~extracellular matrix organization, GO:0045454~cell redox homeostasis, GO:0055114~oxidation-reduction process, GO:0072593~reactive oxygen species metabolic process, GO:0098869~cellular oxidant detoxification, GO:2000255~negative regulation of male germ cell proliferation	GO:0005615~extracellular space, GO:0005623~cell, GO:0005634~nucleus, GO:0005739~mitochondrion, GO:0005790~smooth endoplasmic reticulum, GO:0005829~cytosol, GO:0070062~extracellular exosome	GO:0005515~protein binding, GO:0008379~thioredoxin peroxidase activity, GO:0016209~antioxidant activity, GO:0016491~oxidoreductase activity, GO:0042803~protein homodimerization activity, GO:0051920~peroxiredoxin activity
2967	ERP29	Homo sapiens	GO:0000187~activation of MAPK activity, GO:0001934~positive regulation of protein phosphorylation, GO:0006457~protein folding, GO:0006886~intracellular protein transport, GO:0009306~protein secretion, GO:0010628~positive regulation of gene expression, GO:0010629~negative regulation of gene expression, GO:0043335~protein unfolding, GO:0050709~negative regulation of protein secretion	GO:0005783~endoplasmic reticulum, GO:0005788~endoplasmic reticulum lumen, GO:0005790~smooth endoplasmic reticulum, GO:0009986~cell surface, GO:0016020~membrane GO:0030133~transport vesicle, GO:0042470~melanosome, GO:0070062~extracellular exosome	GO:0003756~protein disulfide isomerase activity, GO:0042803~protein homodimerization activity, GO:0051087~chaperone binding, GO:0042803~protein homodimerization activity, GO:0051087~chaperone binding
3516	KRT10	Homo sapiens	GO:1902235~regulation of endoplasmic reticulum stress-induced intrinsic apoptotic signaling pathway, GO:0030216~keratinocyte differentiation	GO:0005615~extracellular space, GO:0005634~nucleus, GO:0005737~cytoplasm GO:0005882~intermediate filament, GO:0016020~membrane, GO:0070062~extracellular exosome	GO:0030280~structural constituent of epidermis
3304	FTL	Homo sapiens	GO:0006826~iron ion transport, GO:0006879~cellular iron ion homeostasis, GO:0006880~intracellular sequestering of iron ion, GO:0055072~iron ion homeostasis	GO:0005623~cell, GO:0005737~cytoplasm, GO:0005829~cytosol, GO:0008043~intracellular ferritin complex, GO:0016020~membrane, GO:0044754~autolysosome, GO:0070062~extracellular exosome	GO:0005506~iron ion binding, GO:0005515~protein binding, GO:0008199~ferric iron binding, GO:0042802~identical protein binding
1821	ALDH2	Homo sapiens	GO:0005975~carbohydrate metabolic process, GO:0006066~alcohol metabolic process, GO:0006068~ethanol catabolic process, GO:0006069~ethanol oxidation	GO:0005759~mitochondrial matrix, GO:0070062~extracellular exosome	GO:0004029~aldehyde dehydrogenase (NAD) activity, GO:0004030~aldehyde dehydrogenase [NAD(P)+] activity, GO:0009055~electron carrier activity, GO:0016491~Oxidoreductase activity, GO:0016620~oxidoreductase activity, acting on the aldehyde or oxo group of donors, NAD or NADP as acceptor
3008	ECHS1	Homo sapiens	GO:0006635~fatty acid beta-oxidation	GO:0005739~mitochondrion, GO:0005759~mitochondrial matrix, GO:0070062~extracellular exosome	GO:0004300~enoyl-CoA hydratase activity, GO:0005515~protein binding

Table 5. Differences proteins in KEGG pathway

Match ID	Gene Name	Species	KEGG_PATHWAY
2789	ANXA4	Homo sapiens	
3033	PRDX4	Homo sapiens	
2967	ERP29	Homo sapiens	hsa04141: Protein processing in endoplasmic reticulum
3516	KRT10	Homo sapiens	
3304	FTL	Homo sapiens	hsa04978: Mineral absorption
1821	ALDH2	Homo sapiens	hsa00010: Glycolysis/Gluconeogenesis, hsa00040: Pentose and glucuronate interconversions, hsa00053: Ascorbate and aldarate metabolism, hsa00071: Fatty acid degradation, hsa00280: Valine, leucine and isoleucine degradation, hsa00310: Lysine degradation, hsa00330: Arginine and proline metabolism, hsa00340: Histidine metabolism, hsa00380: Tryptophan metabolism, hsa00410: beta-Alanine metabolism, hsa00561: Glycerolipid metabolism, hsa00620: Pyruvate metabolism, hsa01100: Metabolic pathways, hsa01130: Biosynthesis of antibiotics
3008	ECHS1	Homo sapiens	hsa00062: Fatty acid elongation, hsa00071: Fatty acid degradation, hsa00280: Valine, leucine and isoleucine degradation, hsa00310: Lysine degradation, hsa00380: Tryptophan metabolism, hsa00410: beta-Alanine metabolism, hsa00640: Propanoate metabolism, hsa00650: Butanoate metabolism, hsa01100: Metabolic pathways, hsa01130: Biosynthesis of antibiotics, hsa01200: Carbon metabolism, hsa01212: Fatty acid metabolism

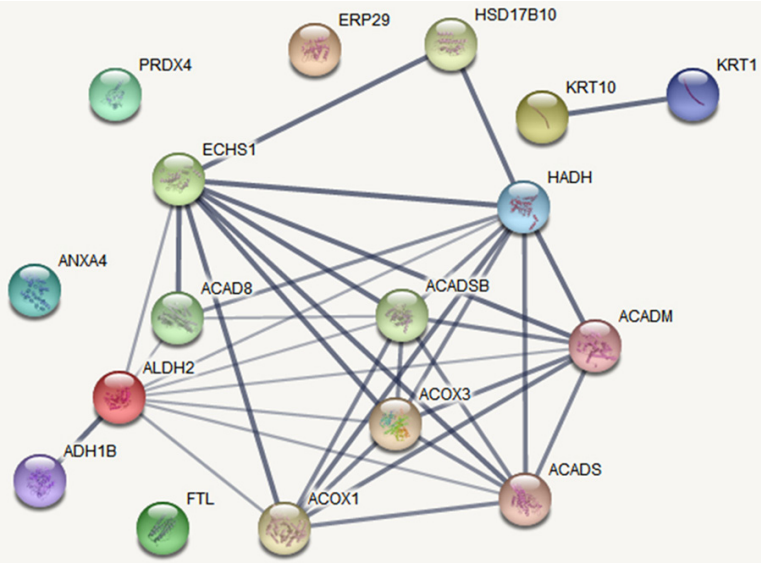

Figure 6. Different proteins in the interaction network.

08. ANXA4, PRDX4, ERP29, KRT10, FTL proteins were independent of the network. ECHS1 and ALDH2 were located in the network and have weak interaction. The thickness of the line between proteins represents the strength of the action. It can be seen from the **Figure 6** that ECHS1 had a strong connection and interaction with other proteins.

As shown in **Table 6**, there were 9 genes involved in the process of small molecule decomposition in protein interaction network. There were 8 genes involved in the process

Table 6. The biological process of differences proteins in network

pathway ID	pathway description	count in gene set	false discovery rate
GO:0044282	small molecule catabolic process	9	1.12e-09
GO:0046395	carboxylic acid catabolic process	8	3.21e-09
GO:0006635	fatty acid beta-oxidation	5	9.61e-07
GO:0019752	carboxylic acid metabolic process	9	3.11e-06
GO:0055114	oxidation-reduction process	9	1.31e-05
GO:0032787	monocarboxylic acid metabolic process	7	3.44e-05
GO:0044281	small molecule metabolic process	11	3.76e-05
GO:0006631	fatty acid metabolic process	6	4.42e-05
GO:0009083	branched-chain amino acid catabolic process	3	0.00028
GO:0006629	lipid metabolic process	8	0.000295
GO:1901575	organic substance catabolic process	9	0.000295
GO:0033539	fatty acid beta-oxidation using acyl-CoA dehydrogenase	2	0.00516
GO:0006069	ethanol oxidation	2	0.0144
GO:0033540	fatty acid beta-oxidation using acyl-CoA oxidase	2	0.0164
GO:0050709	negative regulation of protein secretion	3	0.0316
GO:0006520	cellular amino acid metabolic process	4	0.0463

Table 7. The molecular function of differences proteins in network

pathway ID	pathway description	count in gene set	False discovery rate
GO:0003995	acyl-CoA dehydrogenase activity	6	2.49e-12
GO:0050662	coenzyme binding	7	1.25e-07
GO:0050660	flavin adenine dinucleotide binding	5	2.5e-06
GO:0016491	oxidoreductase activity	8	1.34e-05
GO:0016627	oxidoreductase activity, acting on the CH-CH group of donors	4	4.26e-05
GO:0003857	3-hydroxyacyl-CoA dehydrogenase activity	2	0.005
GO:0003997	acyl-CoA oxidase activity	2	0.005

of carboxylic acid decomposition. There were 5 genes involved in the β oxidation of fatty acids. There were 9 genes involved in the process of carboxylic acid metabolism. There were 9 genes involved in the process of oxidation-reduction. There were 7 genes involved in the process of carboxylic acid metabolism. There were 11 genes involved in the process of small molecule metabolism. There were 5 genes involved in the process of fatty acid x oxidation. There were 6 genes involved in fatty acid metabolism. There were 3 genes involved in branched chain amino acid catabolism. There were 8 genes involved in lipid metabolism. There were 9 genes involved in organic matter catabolism. There were 2 genes involved in ethanol oxidation. There were 2 genes involved in fatty acid oxidation of acyl-CoA oxidase. There were 3 genes involved in the negative regulation of protein secretion. There were 3 genes involved in the negative regulation of protein secretion. There were 4 genes involved in the process of amino acid metabolism of cells. The existence of each biological process was reasonable, FDR<0.05.

As shown in **Table 7**, there were 6 genes related to acyl-CoA dehydrogenase activity in the protein interaction network. There were 7 genes with molecular functions related to coenzyme linkage. There were 5 genes related to the binding of flavin adenine dinucleotide. There were 8 genes related to the activity of oxidoreductase. There were 4 genes related to the activity of oxidoreductase acting on CH-CH bond. There were 2 genes related to the activity of 3-acylhydroxy-coa dehydrogenase. There were 2 genes related to the activity of acyl coenzyme A oxidation. The existence of each molecular function was reasonable, FDR<0.05.

Table 8. The cellular component of differences proteins in network

pathway ID	pathway description	count in gene set	false discovery rate
GO:0005759	mitochondrial matrix	8	2.36e-07
GO:0005739	mitochondrion	9	0.000793
GO:0070062	extracellular exosome	10	0.00285
GO:0044429	mitochondrial part	6	0.00726
GO:0070013	intracellular organelle lumen	11	0.00726
GO:0005782	peroxisomal matrix	2	0.0392
GO:0005790	smooth endoplasmic reticulum	2	0.0392

As shown in **Table 8**, there were 8 genes related to the composition of mitochondrial matrix in the network. There were 9 genes related to the composition of mitochondria. There were 10 genes related to the composition of extracellular matrix. There were 6 genes related to the composition of mitochondrial component. There were 11 genes related to the composition of intracellular subcellular organelle lumen. There were 2 genes related to the composition of peroxidase matrix. There were 2 genes related to the smooth endoplasmic reticulum composition. The existence of each molecular function was reasonable, FDR<0.05.

As shown in **Table 9**, there were 8 genes involved in the fatty acid degradation pathway in the network. There were 7 genes involved in the degradation pathway of valine, leucine and isoleucine. There were 7 genes involved in fatty acid metabolism pathways. There were 10 genes involved in metabolic pathways. There were 3 genes involved in both octyl butyrate metabolism and the PPAR signaling pathway. There were two genes involved in unsaturated fatty acid biosynthesis, fatty acid elongation, alpha linolenic acid metabolism, beta alanine metabolism, propionic acid metabolism, tryptophan metabolism, lysine degradation, or peroxisome pathway. The existence of each pathway was reasonable, FDR<0.05.

Discussion

Silicosis is the earliest described pneumoconiosis due to long-term inhalation of a large amount of dust containing free silica, which is mainly caused by pulmonary fibrosis [19]. Alveolar macrophages (AM) are dust target cells that are activated by endogenous danger signals or pathogen-associated molecules (PAMPs). Activated macrophages can recognize dust phagocytosis and produce reactive oxygen species and nitrogen and some proinflammatory cytokines to kill invading pathogens. Macrophages are constantly activated, constantly producing inflammatory factors, and eventually leading to pulmonary fibrosis [20, 21]. Alveolar macrophages, as targets of dust, play a role in recognizing and swallowing dust, but long-term dust stimulation can damage macrophages, cause them to rupture and disintegrate, which seriously affects the actin function of cells, reduces the number of false feet, and cause the loss of attachment habits of cell wall growth.

Proteins are the executor of physiological functions and the direct embodiment of life phenomena. Compared with the detection of a single biological index, proteomics research has the characteristics of being high throughput, with strong pertinence, systematicness and integration, which greatly increased the complexity of research, and with it the analysis of life phenomena is closer to the real biological functions. This has become the main method used to search for major disease markers with unknown mechanisms. The application of proteomics in silicosis research involves 2-DE and mass spectrometry which were used to analyze the proteins in the serum of the exposed silicosis group and the control group. Eight kinds of serum differential proteins, such as transferrin, glutathione peroxidase, α-2 glycoprotein rich in leucine and tetracycline, were isolated and identified, which enriched the serum protein pool of silicosis and provided the basis for the early diagnosis of silicosis. Bastien Dalzon used two-dimensional gel electrophoresis and mass spectrometry to analyze the toxic mechanism of nanoscale silica on macrophages. It was found that macrophages cultured in different culture medium stimulated silica macrophages with different particle sizes and concentrations, and there were differences in toxicity of different sources of macrophages to the same size and concentration of silica [22, 23]. In this study, two-dimensional gel electrophoresis and time-of-flight mass spectrometry were used to isolate and identify differential proteins in pulmonary alveolar mac-

Table 9. The KEGG pathways of differences proteins in network

pathway ID	pathway description	count in gene set	false discovery rate
00071	Fatty acid degradation	8	1.31e-15
00280	Valine, leucine and isoleucine degradation	7	3.54e-13
01212	Fatty acid metabolism	7	4.53e-13
01100	Metabolic pathways	10	3.23e-07
00650	Butanoate metabolism	3	7.03e-05
03320	PPAR signaling pathway	3	0.00111
01200	Carbon metabolism	3	0.00319
01040	Biosynthesis of unsaturated fatty acids	2	0.00485
00062	Fatty acid elongation	2	0.00509
00592	alpha-Linolenic acid metabolism	2	0.00509
00410	beta-Alanine metabolism	2	0.00679
00640	Propanoate metabolism	2	0.0076
00380	Tryptophan metabolism	2	0.0104
00310	Lysine degradation	2	0.0159
04146	Peroxisome	2	0.036

rophages treated with lung lavage for patients with pulmonary dust deposition, stage I silicosis, stage II silicosis and stage III silicosis. There were two differential proteins between the pulmonary dust deposition group and the stage I silicosis group, PRDX4 and ANXA4. There were five differential proteins between the pulmonary dust deposition group and the stage II silicosis group, which were ERP29, KRT10, FTL, ECHS1 and ALDH2. Bastien Dalzon used two-dimensional gel electrophoresis and mass spectrometry to study the change of core protein of J774 macrophages stimulated by CuO nanoparticles [23]. It was found that FTL, GCLM, HINT1, cGMP and PSMG1 expressed differences in RPMI macrophages and RPMI macrophages cultured in two culture media. Catherine Aude-Garcia [24] analyzed the toxic effect of nano zinc oxide particles on macrophages by proteomic technology. It was found that there were differences in the effects of ERP29, GCLM, MYD88, RUVBL2 and other proteins when zinc oxide and zirconia particles stimulated J774 macrophages. The results of this study were not exactly in line with the findings of Bastien Dalzon and Catherine Aude-Garcia. This may be due to different biological samples in the study. The biological samples they studied were sera from patients with silicosis and macrophages from J774. The biological samples in this study were alveolar macrophages from patients with silicosis. Different experimental results can be obtained by using different research samples.

At the beginning of the study design, we considered the sensitivity of proteomics and the influence of many factors. The most important thing was that the alveolar macrophages were considered as the target cells of dust. In order to study the real mechanism of the occurrence and development of silicosis, we finally selected the macrophages in the alveolar lavage fluid of silicosis patients as biological samples. Silicosis was different from pneumoconiosis. Pneumoconiosis is a reversible disease. It is possible for patients to recover to a 'normal person' when they are out of contact with dust. Therefore, those who had not been assessed as having pneumoconiosis were selected as the control group. In the experimental process, for the individual differences in the population, the selection and exclusion criteria were strictly controlled. Macrophages were separated from the lung lavage fluid of silicosis patients by two-dimensional gel electrophoresis. Every protein sample of every silicosis patient was completed by two-dimensional gel electrophoresis, instead of mixing every protein phase of silicosis into a protein pool for two-dimensional gel electrophoresis. In this way, the influence of individual differences on the whole cycle samples was avoided. Two-dimensional gel electrophoresis was used to separate the macrophage protein in each alveolar lavage fluid, which increased the repeatability of the experiment and ensured the quality of the experimental results.

Bruker's New ultrafleXtreme reflective tandem matrix-assisted laser desorption time-of-flight mass spectrometry was compared with Swiss-Prot57.15 database search, which could find the co-identification of membrane adhesion protein A4 (ANXA4), recombinant human peroxidase 4 (PRDX4), endoplasmic retinin 29 (ERP29), keratin type I cytoskeleton (KRT10), ferritin light chain (FTL), mitochondrial enoyl-CoA hydratase (ECHS1), and mitochondrial acetaldehyde dehydrogenase (ALDH2) as seven the proteins identified in this study. The remaining 16 samples were detected by mass spectrometry, 11 of which did not reach the detection limit of the mass spectrometry, that is, no detection results. The detection results of the remaining 5 samples were cytoskeletal proteins. There were 2 differential proteins between the pulmonary dust deposition group and the stage I silicosis group, 5 differential proteins between the pulmonary dust deposition group and the stage II silicosis group, and there were no differential proteins between the pulmonary dust deposition group and the stage III silicosis group. The ECHS1 protein with a match ID of 3008 was different between the pulmonary dust deposition group and stage III silicosis group, the pulmonary dust deposition group and stage II silicosis group. ECHS1 protein is likely to be a key protein affecting the development of silicosis.

After identifying the differential proteins by mass spectrometry and obtaining protein information, bioinformatics was used to perform in-depth analysis on GO, KEGG Pathway, and PPI. Bioinformatics was first proposed by Dutch theoretical biologists Paulien Hogeweg and Ben Hesper in 1978. It was a conceptual biology in the field of macromolecules. It was a medical science, biology, an interdisciplinary discipline of genomics, genetics, physiology, mathematics, and computer science for understanding and organizing information related to biological macromolecules [11]. According to bioinformatics analysis, the RPKM value of the three proteins ALDH2 [25], ERP29, and FTL in the lung tissue were around 50. The RPKM values of the three proteins ECSC1, ANXA4, and PRDX4 in the lung tissue were 15-25. Interestingly, KRT10 only exists in skin tissue, and the detection of KRT10 in this experiment suggests that alveolar macrophages may be keratinized. From the results of protein distribution, ALDH2, ERP29, and FTL were more distributed in lung tissues, which may be more related to the progress of silicosis, and more likely to be the key proteins for the development of silicosis.

According to bioinformatics analysis, the occurrence and development of silicosis may be due to one or more proteins mentioned above, and it may also be related to one or more signal pathways. This experiment was a preliminary study on the differential proteins of macrophages in different stages of silicosis [26]. If the key proteins affecting the development of silicosis need to be confirmed, a large number of validation experiments were needed to verify the stable expression of seven proteins, namely ANXA4, PRDX4, ERP29, KRT10, FTL, ECHS1 and ALDH2, in silicosis patients. These seven differential proteins were considered to be the key proteins in the carcinogenesis and development of cancer. There was no exact functional pathway between PRDX4 and ANXA4. ANXA4 was a member of membrane mucin family. PRDX4 was the only known secretory protein of peroxisome reductase family. The existence of PRDX4 and ANXA4 in the pneumoconiosis group and the silicosis group suggest that dust may affect the membrane movement of macrophages, regulate the secretion of peroxisome reductase and damage macrophages and alveoli in the early stage of silicosis [27-29]. ECHS1 and ALDH2 were mitochondrial proteins, which were involved in fatty acid degradation and amino acid metabolism, such as valine, leucine, isoleucine, lysine and tryptophan [28, 29]. ERP29 is an endoplasmic reticulum protein, which can change the transformation of mesenchymal epithelial cells [30, 31]. FTL participates in the process of iron metabolism and inflammation [32, 33]. KRT10 can make cells keratinize. These proteins were present in the lung dust pulmonary dust deposition group and stage I silicosis group suggest that dust entering macrophages can cause subcellular organ damage. Dust constantly stimulates subcellular organelles to cause amino acid metabolism, where fatty acid metabolism disorders cause macrophages to keratinize, and lose phagocytosis. According to the changes of alveolar macrophages, it was inferred that with the occurrence and development of silicosis the ability of macrophages to recognize dust decreases with the progress of silicosis. The reduction of

secreted redox proteins puts the lungs in a state of oxidative stress and inflammation. The dust entering the alveolar macrophages destroys important subcellular structures such as mitochondria and endoplasmic reticulum. Disorder of amino acid metabolism and fatty acid metabolism led to loss of phagocytic function of alveolar macrophages, which eventually led to pulmonary fibrosis.

In summary, based on protein omics and bioinformatics analysis, this research group concluded that the seven proteins (ANXA4, PRDX4, ERP29, KRT10, FTL, ECHS1, and ALDH2) are proteins related to the occurrence and development of silicosis in the 31 selected silicotic patients. These protein expressions of PRDX4, ANXA4, ERP29, FTL, and KRT10 promote the development of pneumoconiosis. The expression levels of ECHS1 and ALDH2 are changed due to pneumoconiosis. These proteins were the main proteins affecting the occurrence and development of silicosis, and provided reference basis for the research on the occurrence and development mechanism of silicosis in the future.

Conclusion

Application of differential proteomics and time-of-flight mass spectrometry revealed that the proteins associated with silicosis development in alveolar macrophages were ANXA4, PRDX4, ERP29, KRT10, FTL, ECHS1, and ALDH2; which enriched the knowledge of alveolar macrophage proteins that occur in silicosis.

Bioinformatics analysis results of the main mechanisms of alveolar macrophages in silicosis: fatty acid metabolism, MAPK activity regulation, oxidative stress, Notch signaling pathway, and interleukin-8 secretion negative regulation.

The ECHS1 protein with Match ID 3008 was different between the pulmonary dust deposition group and stage I silicosis group, the pulmonary dust deposition group and stage II silicosis group. ECHS1 protein is likely to be a key protein in the development of silicosis.

Acknowledgements

We would like to thank all participants in this study. This work was supported by the grants from the Natural Science Foundation of Hebei Province (Project number: H2017209195) and Key projects of Hebei Provincial Department of Education (Project number: ZD2018226).

Disclosure of conflict of interest

None.

Address correspondence to: Dr. Fuhai Shen, Hebei Province Key Laboratory of Occupational Health and Safety for Coal Industry, School of Public Health, North China University of Science and Technology, 21 Bohai Dadao, Tangshan 063210, Hebei, China. E-mail: shfh600@163.com; Huisheng Qi, Tangshan City Workers' Hospital, 27 Wenhua Road, Tangshan 063000, Hebei, China. E-mail: qhs197323@163.com

References

[1] Chen J, Yao Y, Su X, Shi Y, Song X, Xie L, You J, Tian L, Yang L, Fang A and Xiong J. Comparative RNA-Seq transcriptome analysis on silica induced pulmonary inflammation and fibrosis in mice silicosis model. J Appl Toxicol 2018; 38: 773-782.

[2] Kato K, Zemskova MA, Hanss AD, Kim MM, Summer R and Kim KC. Muc1 deficiency exacerbates pulmonary fibrosis in a mouse model of silicosis. Biochem Biophys Res Commun 2017; 493: 1230-1235.

[3] Schoening JM, Corner LAL, Messam LLM, Cassidy JP and Wolfe A. Environmental dust inhalation in the European badger (meles meles): systemic distribution of silica-laden macrophages, pathological changes, and association with Mycobacterium bovis infection status. PLoS One 2018; 13: e0190230.

[4] Wang X, Xu K, Yang XY, Liu J, Zeng Q and Wang FS. Upregulated miR-29c suppresses silica-induced lung fibrosis through the Wnt/β-catenin pathway in mice. Hum Exp Toxicol 2018; 37: 944-952.

[5] Costa C, Ascenti G, Scribano E, D'Angelo T, Gaeta M, Fenga C, Blandino A and Mazziotti S. CT patterns of pleuro-pulmonary damage caused by inhalation of pumice as a model of pneumoconiosis from non-fibrous amorphous silicates. Radiol Med 2016; 121: 19-26.

[6] Quail MT. Overview of silica-related clusters in the united states: will fracking operations become the next cluster? J Environ Health 2017; 79: 20-27.

[7] Xue C, Wu N, Li X, Qiu M, Du X and Ye Q. Serum concentrations of Krebs von den Lungen-6, surfactant protein D, and matrix metalloproteinase-2 as diagnostic biomarkers in patients

with asbestosis and silicosis: a case-control study. BMC Pulm Med 2017; 17: 144.
[8] Zhang L, Hao C, Li J, Qu Y, Bao L, Li Y, Yue Z, Zhang M, Yu X, Chen H, Zhang J, Wang D and Yao W. Bioinformatics methods for identifying differentially expressed genes and signaling pathways in nano-silica stimulated macrophages. Tumour Biol 2017; 39: 1010428317709284.
[9] Aslam B, Basit M, Nisar MA, Khurshid M and Rasool MH. Proteomics: technologies and their applications. J Chromatogr Sci 2017; 55: 182-196.
[10] Helmig S, Lochnit G and Schneider J. Comparative proteomic analysis in serum of former uranium miners with and without radon induced squamous lung cancer. J Occup Med Toxicol 2019; 14: 9.
[11] Livigni A, O'Hara L, Polak ME, Angus T, Wright DW, Smith LB and Freeman TC. A graphical and computational modeling platform for biological pathways. Nat Protoc 2018; 13: 705-722.
[12] The Gene Ontology Consortium. The gene ontology resource: 20 years and still GOing strong. Nucleic Acids Res 2019; 47: D330-D338.
[13] Kanehisa M, Furumichi M, Tanabe M, Sato Y and Morishima K. KEGG: new perspectives on genomes, pathways, diseases and drugs. Nucleic Acids Res 2017; 45: D353-D361.
[14] Chen S, Pan S, Wu H, Zhou J, Huang Y, Wang S and Liu A. ICAM1 regulates the development of gastric cancer and may be a potential biomarker for the early diagnosis and prognosis of gastric cancer. Cancer Manag Res 2020; 12: 1523-1534.
[15] Lipinski S, Pfeuffer S, Arnold P, Treitz C, Aden K, Ebsen H, Falk-Paulsen M, Gisch N, Fazio A, Kuiper J, Luzius A, Billmann-Born S, Schreiber S, Nuñez G, Beer HD, Strowig T, Lamkanfi M, Tholey A and Rosenstiel P. Prdx4 limits caspase-1 activation and restricts inflammasome-mediated signaling by extracellular vesicles. EMBO J 2019; 38: e101266.
[16] Chaiyawat P, Pruksakorn D, Pipatwattana P, Phanphaisarn A, Teeyakasem P, Klangjorhor J and Settakorn J. Endoplasmic reticulum protein 29 (ERp29) as a novel prognostic marker and tumor suppressor in osteosarcoma. J Bone Oncol 2019; 16: 100233.
[17] Xu Y, Sui L, Qiu B, Yin X, Liu J and Zhang X. ANXA4 promotes trophoblast invasion via the PI3K/Akt/eNOS pathway in preeclampsia. Am J Physiol Cell Physiol 2019; 316: C481-C491.
[18] Gao L, Dou J, Zhang B, Zeng J, Cheng Q, Lei L, Tan L, Zeng Q, Ding S, Guo A, Cheng H, Yang C, Luo Z and Lu J. Ozone therapy promotes the differentiation of basal keratinocytes via increasing Tp63-mediated transcription of KRT10 to improve psoriasis. J Cell Mol Med 2020; 24: 4819-4829.
[19] Mielke S, Taeger D, Weitmann K, Brüning T and Hoffmann W. Influence of quartz exposure on lung cancer types in cases of lymph node-only silicosis and lung silicosis in German uranium miners. Arch Environ Occup Health 2018; 73: 140-153.
[20] Vanhée D, Gosset P, Boitelle A, Wallaert B and Tonnel AB. Cytokines and cytokine network in silicosis and coal workers' pneumoconiosis. Eur Respir J 1995; 8: 834-842.
[21] Kamal AHM, Chakrabarty JK, Udden SMN, Zaki MH and Chowdhury SM. Inflammatory proteomic network analysis of statin-treated and lipopolysaccharide-activated macrophages. Sci Rep 2018; 8: 164.
[22] Zhao L, Gao Y, Yang Y, Wei Y, Li Y, Feng H, Wei W, Ding Y and Sun D. Serum proteomic profiling analysis of chronic arsenic exposure by using SELDI-TOF-MS technology. Toxicol Lett 2010; 195: 155-160.
[23] Dalzon B, Diemer H, Collin-Faure V, Cianférani S, Rabilloud T and Aude-Garcia C. Culture medium associated changes in the core proteome of macrophages and in their responses to copper oxide nanoparticles. Proteomics 2016; 16: 2864-2877.
[24] Aude-Garcia C, Dalzon B, Ravanat JL, Collin-Faure V, Diemer H, Strub JM, Cianferani S, Dorsselaer AV, Carrière M and Rabilloud T. A combined proteomic and targeted analysis unravels new toxic mechanisms for zinc oxide nanoparticles in macrophages. J Proteomics 2016; 134: 174-185.
[25] Kuroda A, Hegab AE, Jingtao G, Yamashita S, Hizawa N, Sakamoto T, Yamada H, Suzuki S, Ishii M, Namkoong H, Asakura T, Ozaki M, Yasuda H, Hamamoto J, Kagawa S, Soejima K and Betsuyaku T. Effects of the common polymorphism in the human aldehyde dehydrogenase 2 (ALDH2) gene on the lung. Respir Res 2017; 18: 69.
[26] Au Yeung SL, Jiang C, Cheng KK, Adab P, Lam KB, Liu B, Zhang W, Lam TH, Leung GM and Schooling CM. Aldehyde dehydrogenase 2-a potential genetic risk factor for lung function among southern Chinese: evidence from the Guangzhou biobank cohort study. Ann Epidemiol 2014; 24: 606-611.
[27] Wang HQ, Du ZX, Liu BQ, Gao YY, Meng X, Guan Y and Zhang HY. TNF-related apoptosis-inducing ligand suppresses PRDX4 expression. FEBS Lett 2009; 583: 1511-1515.
[28] Marzony ET, Ghanei M and Panahi Y. Oxidative stress and altered expression of peroxiredoxin genes family (PRDXS) and sulfiredoxin-1 (SRXN1) in human lung tissue following expo-

sure to sulfur mustard. Exp Lung Res 2016; 42: 217-226.
[29] Hwang JA, Song JS, Yu DY, Kim HR, Park HJ, Park YS, Kim WS and Choi CM. Peroxiredoxin 4 as an independent prognostic marker for survival in patients with early-stage lung squamous cell carcinoma. Int J Clin Exp Pathol 2015; 8: 6627-35.
[30] Gao J, Zhang Y, Wang L, Xia L, Lu M, Zhang B, Chen Y and He L. Endoplasmic reticulum protein 29 is involved in endoplasmic reticulum stress in islet beta cells. Mol Med Rep 2016; 13: 398-402.
[31] Bambang IF, Lee YK, Richardson DR and Zhang D. Endoplasmic reticulum protein 29 regulates epithelial cell integrity during the mesenchymal-epithelial transition in breast cancer cells. Oncogene 2013; 32: 1240-1251.
[32] Rosager AM, Sørensen MD, Dahlrot RH, Hansen S, Schonberg DL, Rich JN, Lathia JD and Kristensen BW. Transferrin receptor-1 and ferritin heavy and light chains in astrocytic brain tumors: expression and prognostic value. PLoS One 2017; 12: e0182954.
[33] Chen S, Yuan J, Yao S, Jin Y, Chen G, Tian W, Xi J, Xu Z, Weng D and Chen J. Lipopolysaccharides may aggravate apoptosis through accumulation of autophagosomes in alveolar macrophages of human silicosis. Autophagy 2015; 11: 2346-2357.